Chromium Removal and Sorption Mechanism from Aqueous Solutions by Wine Processing Waste Sludge

Cheng-Chung Liu,[†,‡] Ming-Kuang Wang,*[,†] Chyow-San Chiou,[‡] Yuan-Shen Li,[‡] Yu-An Lin,[§] and Shu-Shan Huang[‡]

Department of Agricultural Chemistry, National Taiwan University, Taipei, Taiwan 106, and Departments of Environmental Engineering and Animal Science, National Ilan University, Ilan, Taiwan 260

Wine processing waste sludge (WPWS) has been shown to be an effective sorbent for the sorption of heavy metals (i.e., chromium and nickel), but the mechanism of removal of hexavalent chromium [Cr(VI)] by WPWS remains obscure. The aims of this study were to determine the effects of temperature, initial concentration of Cr(VI), and particle size on the removal Cr(VI) using WPWS. The characteristics of WPWS were determined, and sorption mechanism studies were also performed. The WPWS used was a deposit mixture containing considerable quantities of chemical coagulation as well as activated sludge precipitation from the settling basins of a wastewater treatment plant. Differential scanning calorimetry (DSC) analysis revealed that the WPWS comprised abundant labile carbohydrates and few aromatic structures. According to the IR spectrum, carboxylic groups were the most important functional group in WPWS, interacting with chromium species by protonation and redox reaction. All kinetic experiments were conducted at an initial pH of 2.0, and all of them had reached steady state within 240 min. The final pH values of the suspensions were approximately 4.2, and the increase of the pH caused low Cr removal. In addition, about 2−18% of the Cr(III) remained in the liquid phase. The Cr removal percentage increased with increasing temperature (i.e., 14−25%), but it was less affected by particle size (17−22%). All kinetic data obtained from different conditions showed good compliance with a pseudo-second-order model, and the rate constant k_2 was found to range from 0.032 to 0.074 g mg^{-1} min^{-1}. Some of the Cr(VI) ions were reduced to Cr(III) ions as a result of oxidation of organic components in WPWS, as indicated by monitoring using the X-ray absorption near-edge spectroscopic (XANES) technique.

Introduction

Chromium commonly occurs in a trivalent, Cr(III), or hexavalent, Cr(VI), state in natural environments. A small amount of Cr(III) is an essential nutrient for human beings and works with insulin to metabolize carbohydrates, fats, and proteins.[1] However, Cr(VI) exhibits a toxicity 500 times that of Cr(III).[2] Cr(VI) compounds are well-known human carcinogens, and exposure to Cr(VI) by inhalation, touch, and ingestion can induce headaches, coughing, impaired breathing, ulcerated skin, corneal damage, nausea, vomiting, gastrointestinal convulsions, etc. The sources of Cr(VI) are various industries, such as plating, texture dyeing, and paper manufacturing, as well as the production of batteries, plastics, refrigerators, alloys, and paints. Cr(VI) is usually found in bottom sediments of lakes and rivers, tannery wastes, sewage sludge, aerosols, and hazardous waste sites.[3]

In chromium-plating industry effluent, the concentration of Cr(VI) is in the range of 15−300 mg L^{-1},[4] occasionally exceeding 960 mg L^{-1}.[5] At an extreme level, effluents from tannery factories have been reported to contain 1300−2500 mg L^{-1} of Cr(VI).[6] At Cr(VI) concentrations of less than 10 mM, CrO_4^{2-} is the predominant species above pH 6.5, H_2CrO_4 predominates only if the pH is below 0.9, and $HCrO_4^-$ predominates in the intermediate pH range of 0.9−6.5. For total concentrations of Cr(VI) greater than 10 mM, $HCrO_4^-$ polymerizes to form $Cr_2O_7^{2-}$ under acidic conditions.[7] Conventional methods for removing heavy metals from wastewater include reverse osmosis, ion exchange, chemical precipitation, chemical oxidation and reduction, electrocoagulation, and sorption.[5] In sorption treatment, activated carbon, including Cr(VI) from wastewater, is employed extensively as a sorbent for the removal of toxic metals.[8,9] In recent years, some industrial and agricultural wastes, such as fly ash,[10,11] activated sludge,[12] blast furnace fluedust,[13] red mud,[14] and distillery sludge,[15] have been examined for the possibility of replacing expensive activated carbon in this application.

Bioremediation is an effective and economical method for removing various toxic heavy metals by using residues of higher plants[16−20] and dead biomass of microbes,[21−25] including bacteria, fungi, yeast, and algae. The mechanisms of removing dissolved toxic metal ions by biosorption mainly depend on the interactions between the metal ions and specific functional groups, such as phenolic, alcoholic, carboxylic, and amino groups, associated with the cell walls of biosorbents. The Cr(VI) anion species could be bound to the protonated active sites of biosorbents at low pH. In addition, reduction of Cr(VI) to Cr(III) could be conducted on biosorbent surfaces under conditions of extreme acidity, high Cr(VI) concentration, and high temperature.[26−28] Wine processing waste sludge (WPWS), a deposit mixture comprising considerable quantities of activated sludge and a great deal of plant debris, could be considered as a biosorbent. This study was aimed at examining the capability of WPWS as a sorbent for Cr(VI) and the mechanism for removing Cr(VI) from aqueous solutions using WPWS as a sorbent.

* To whom correspondence should be addressed. Tel.: (0118862) 3366-4808. Fax: (0118862) 2366-0751. E-mail: mkwang@ntu.edu.tw.

[†] National Taiwan University.

[‡] Department of Environmental Engineering, National Ilan University.

[§] Department of Animal Science, National Ilan University.

10.1021/ie060978q CCC: $33.50
Published on Web 11/29/2006

Experimental Methods

Materials. Wine processing waste sludge was supplied by the Ilan Wine-Processing Company, Ilan, Taiwan. This sludge was a deposit mixture, containing considerable quantities of activated sludge, from the final settling basins of wastewater treatment plants. The wastewater came from the domestic wastewater of workers, rainwater, and the washing of wine-processing machines and wine-making ingredients. After being dried in air, the WPWS was crushed and sieved into four particle sizes with average diameters of 0.297, 0.149, 0.105, and <0.105 mm, represented as 50−100, 100−140, 140−200, and >200 mesh, respectively. The quantity of WPWS with 100−140 mesh accounted for about 50% of the total. The sieved WPWS was rinsed with doubly deionized water (DDW), air-dried again, and then stored in a refrigerator at 4 °C.

Methods. The pH of WPWS suspensions at a 1:5 WPWS-to-water ratio was determined by a pH meter (TitraLab TIM-865 Titration Manager). An energy-dispersive spectrometer (EDS, Kevex level 4) was employed to examine the major elemental constituents of WPWS. Total nitrogen and organic carbon analyses were carried out with an automatic elemental analysis machine (Heraeus VarioEL-III). All chemicals used were of analytical reagent grade and were obtained from RDH Co. (Germany). The stock solution of Cr(VI) (100 mg L^{-1}) was prepared from $K_2Cr_2O_7$ using DDW and was diluted to the desired concentrations. A 1×10^{-2} M $NaClO_4$ solution was employed to control the ionic strength. From earlier reports, Cr(VI) removal is the highest at pH 1.5−2.0.[16−25] Thus, most experiments in this study were carried out using Cr(VI) solutions with an initial pH of 2.0.

(i) X-ray Diffraction (XRD) Analysis. WPWS was treated with 35% H_2O_2 water to remove organic matter. Then, this air-dried sample was X-rayed at 25 °C. The oriented samples were examined with Cu Kα radiation using a Rigaku Geigerflex X-ray diffractometer. The XRD patterns were recorded in the range of 2−60°(2θ) at a scanning speed of 1° (2θ) min^{-1}.

(ii) Thermal Analysis. To obtain further information regarding WPWS characteristics, the WPWS was subjected to differential scanning calorimetry (DSC), thermogravimetry (TG), and differential thermogravimetry (DTG) analyses. The DSC analyses were conducted using a Netzsch DSC 404 differential scanning calorimeter, calibrated for temperature and enthalpy by melting indium and a sample weighing 12.9 mg on a small γ-aluminum oxide pan. The DSC thermograms were recorded from 40 to 650 °C at a ramp of 10 °C min^{-1} in a nitrogen stream of 50 mL min^{-1}. The positive sign of the DSC curve (mW mg^{-1}) indicated that the reaction in the spectrum was endothermic. The TG and DTG analyses were conducted using an AutoTGA 2950HR V5.4A instrument at a heating rate of 10 °C min^{-1} from 30 to 300 °C, in a nitrogen atmosphere (flow rate 100 mL min^{-1}), for a sample with a weight of 8.7 mg. The measurements were also done in duplicate.

(iii) IR Analysis. The predominant functional groups of WPWS were analyzed using an infrared spectrometer (Galactic Industries Corp. BIO-RAD Fis-7) by preparing the sludge pellets in KBr. To obtain further information on the characteristics of the relevant functional groups, samples were pretreated at temperatures of 25, 250, 350, and 550 °C for 24 h before the transparent KBr pellets were made.

(iv) Kinetic Experiments and Model. To perform the kinetic experiments, 1.0 g of WPWS was added individually to a series of 100-mL samples of $K_2Cr_2O_7$, at an initial pH of 2.0 as monitored by pH meter, with various WPWS particle sizes (50−100, 100−140, 140−200, and >200 mesh), initial Cr(VI) concentrations (100, 75, 50, and 25 mg L^{-1}), and temperatures (10, 30, and 50 °C). The suspensions were mixed vigorously with a mechanical shaker for between 1.5 min and 4 h. At the end of each time interval, samples of each suspension were retrieved quickly and filtered through 0.45-μm Millipore filters. Analysis of the total chromium concentration, denoted Cr(T), was performed using an flame atomic absorption spectrophotometer equipped with a high-temperature burner and N_2O gas as the oxidant. The Cr(VI) concentrations of the filtrates were analyzed by the 1,5-diphenylcarbazide method.[29] The Cr(III) concentration was obtained by subtracting the Cr(VI) concentration from the total concentration, Cr(T). All experiments were performed in triplicate.

The sorption kinetics of Cr by WPWS at different operating temperatures, initial Cr(VI) concentrations, and WPWS particle sizes were fitted using both pseudo-first-order and pseudo-second-order sorption equations.[30] The pseudo-first-order equation was

$$\log(q_e - q_t) = \log q_e - \frac{k_1}{2.303}t$$

where k_1 (min^{-1}) is the rate constant, q_t (mg g^{-1}) denotes the amount adsorbed at time t (min), and q_e (mg g^{-1}) is the amount adsorbed at equilibrium. The sorption rate constant, k_1, can be determined by plotting $\log(q_e - q_t)$ against t.

The pseudo-second-order equation can be written as

$$\frac{t}{q_t} = \frac{1}{k_2 q_e^2} + \frac{1}{q_e}t$$

where k_2 (g mg^{-1} min^{-1}) is the rate constant. k_2 and q_e can be obtained from the intercept and slope of a plot of t/q_t against t.

(v) X-ray Absorption Near-Edge Structure (XANES) Studies. X-ray absorption near-edge structure (XANES) can be employed to provide information about the oxidation state of Cr atoms binding to WPWS.[31] When the incident photon energy, below the absorption edge, is scanned across a core electron resonance, relatively little absorption intensity is observed above the baseline. When the photon energy is increased until it is large enough to excite a bound electron out of its orbital, incident X-rays are strongly absorbed.[32] Then, a sharp step-like increase occurs in the absorption cross section.[33] Analysis of the characteristics of these resonances, including the shape, intensity, and energy position, provides information about the valence state, coordination geometry, and effective charge of the excited atom. In general, the first inflection point of the absorption edge is used as a representative value for its energy position.[34] The appearance of a preedge peak can be taken as an indicator of the presence of Cr(VI). In contrast, the spectra of Cr(III) compounds do not exhibit any preedge peak. The Cr(VI) preedge absorption is attributed to the transition of 1s electrons to the empty 3d orbital. This transition is permitted because of the lack of a center of inversion symmetry in the Cr(VI) tetrahedral structure, but it is not allowed in the octahedral Cr(III) structure.[35]

In this study, five Cr-loaded WPWS samples with different reaction periods were subjected to XANES analysis. Each sample was prepared by mixing 1.0 g of WPWS (<0.105 mm) with 100 mL of $K_2Cr_2O_7$ solution containing 100 mg L^{-1} Cr and having a pH of 2.0 at 30 °C and was then sampled at each of the following reaction intervals: 1.5, 3, 9, 15, and 240 min. All samples were packed into aluminum holders of 2-mm thickness and sealed with Kapton tape. The Cr K-edge (5989 eV) spectra were recorded in fluorescence mode on beamline

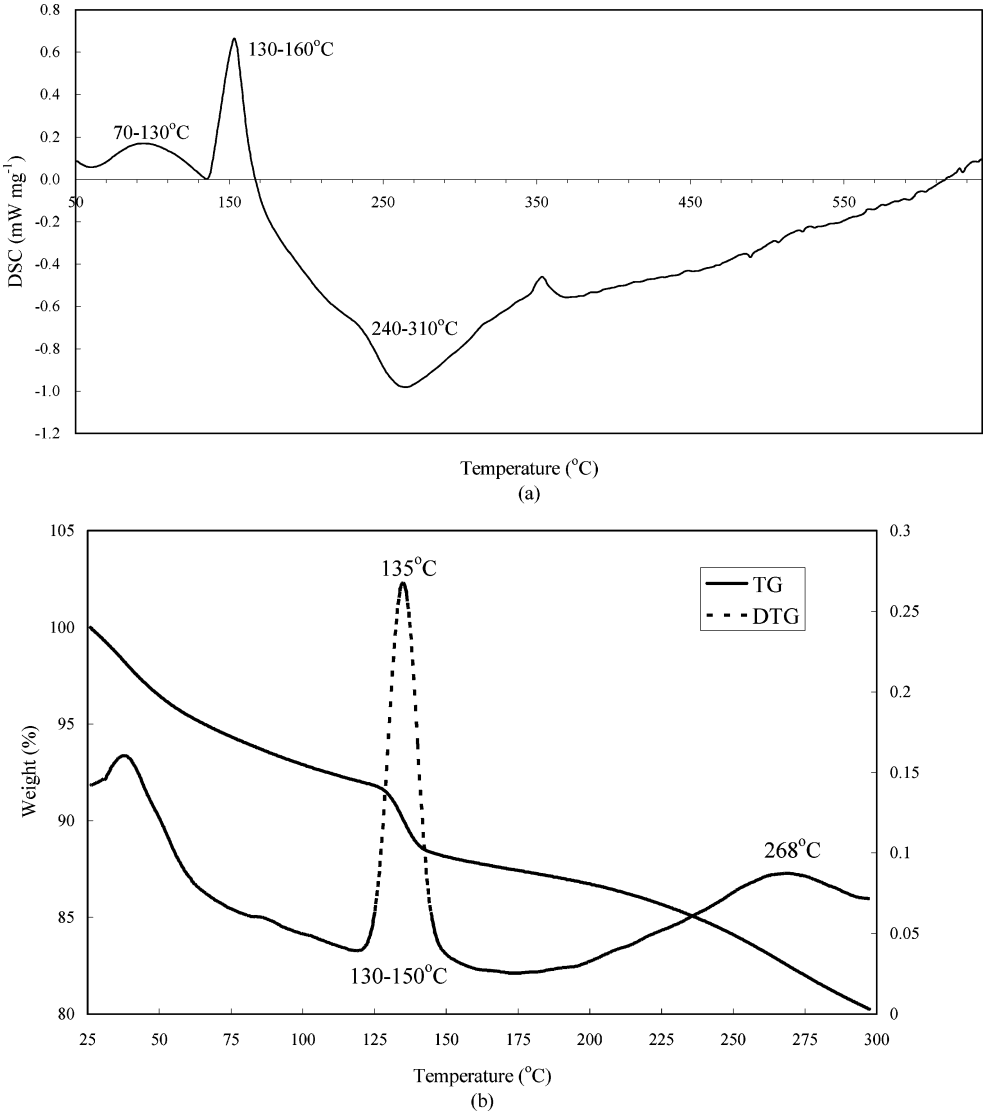

Figure 1. (a) DSC and (b) TG−DTG curves of WPWS.

17C at the National Synchrotron Radiation Research Center (NSRRC) in Hsin-Chu, Taiwan. The calibration for all spectra was undertaken against the edge position (5989 eV) using a pure Cr(0) foil. The experiments were performed in the Cr K-edge, ranging from 5789 to 6989 eV, at ambient temperature. The XANES data were analyzed using the Original 7.0 software package.

Results and Discussion

Components and Characteristics of WPWS. The organic and nitrogen contents of WPWS were found to be 38.2% and 169.3 cmol kg^{-1}, respectively. This high organic matter content of WPWS offers a tremendous number of sorption sites. The chemical composition (cmol kg^{-1}) of WPWS determined by EDS was as follows: potassium, 24.2; calcium, 226.7; magnesium, 36.2; iron, 470.4; aluminum, 93.9; manganese, 1.7; phosphorus, 226.1; sulfur, 145.7; and silicon, 282.9. The pH of WPWS was 7.8, and this value is probably associated with a high calcium content. Calcium, iron, and aluminum came from the flocculating agents for the wastewater treatments. Only small amounts of quartz were identified in the XRD spectrum (data not shown). The quartz might originate from the diatomite employed in the dehydration process for raw sludge.

As seen in Figure 1a, the broad endothermic peak at 70−130 °C represents the vaporization of water adsorbed on the surface and in the large pores of WPWS. The intense broad exothermic peak at 240−310 °C can be attributed to the degradation of the carbohydrates and decarboxylation of carboxyl groups.[36] However, no peak appears from 440 to 540 °C, revealing that the composition of WPWS lacks stable materials such as aromatic structures.[37] An intense DSC endothermic peak appearing at 130−160 °C was once of great concern to us, and few studies had paid attention for it. Abou-Mesalam[38] attributed the prominent endothermic peak at 150 °C to the free adsorbed water of silicoantimonate. The TG and DTG curves shown in Figure 1b indicate that there is a defined weight loss at 130−150 °C (i.e., 135 °C). Thus, we speculate that the mass of water adsorbed firmly in the small pores of WPWS would escape in this temperature range.

A broad IR absorption band at 1020−1150 cm^{-1}, without apparent change during all of the heat treatments, can be assigned to be the Si−O vibration[39] of quartz (Figure 2). An intense absorption band at 1380 cm^{-1} is present at 25 °C that disappears after heat treatments above 250 °C. It can be attributed to the C−H stretch of alkyl.[40] Another intense absorption band appearing around 1650 cm^{-1} can be attributed

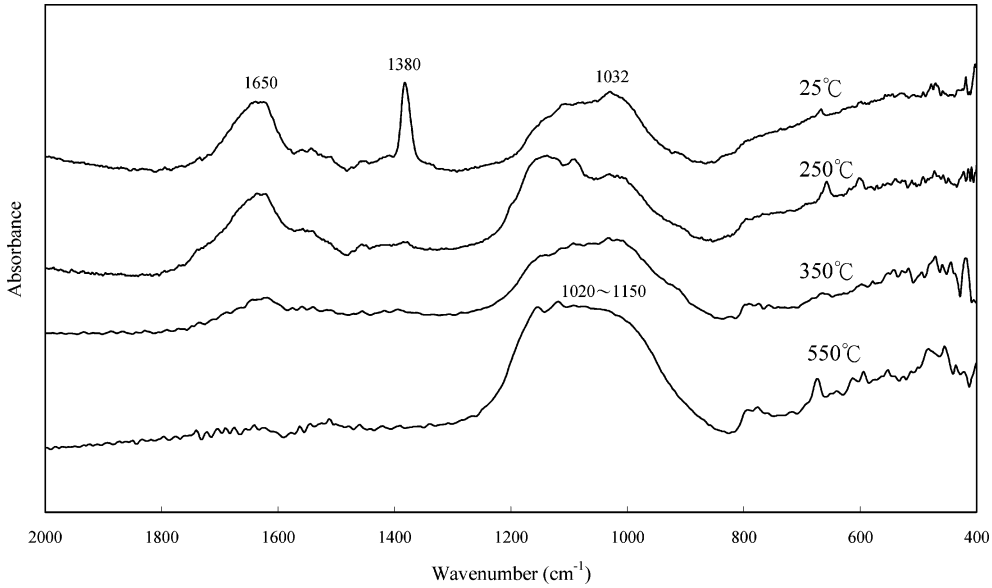

Figure 2. IR spectra of WPWS heated at different temperatures.

Table 1. Removal Ratios of Total Chromium [Cr(T)] and Ratios of Cr(III) Remaining in the Liquid Phase at Different Temperatures, Initial Cr(VI) Concentrations, and Particle Sizes of WPWS at Steady State

temperature (°C)	Cr(T) removal (%)	Cr(III) liquid (%)	concentration (mg L^{-1})	Cr(T) removal (%)	Cr(III) liquid (%)	particle size (mesh)	Cr(T) removal (%)	Cr(III) liquid (%)
10	14	2	25	36	18	50−100	17	4
30	18	5	50	24	10	100−140	18	5
50	25	6	75	21	7	140−200	19	5
			100	18	5	>200	22	5

to the carbonyl stretch of ionized coordinated COO^- groups.[41] Thus, we consider the ionized coordinated COO^- group as the prominent type of carboxylate functionality present on native WPWS. After the 250 °C treatment, the absorption band at 1650 cm^{-1} still shows an approximate absorption band, but this band becomes markedly weakened at 350 °C and disappears entirely at 550 °C. The results reveal that the carboxyl groups of WPWS are broken down quickly when the temperature exceeds 250 °C. No apparent IR absorption band is present in the 1516 cm^{-1} region, which is the typical region for aromatic ring C−C stretching.[42] This fact indicates that there are few aromatic structures in WPWS,[43] in agreement with the DSC analyses. Therefore, WPWS performs as a labile and easily decomposed material. In short, carboxyl groups are the predominant functional groups and the main sites in WPWS for interaction with Cr.

Sorption Kinetics. All reactions reached steady state within 240 min, during which the pH of the suspensions increased gradually from an initial value of 2.0 to around 4.2. From the experimental results, it is postulated that, when the reactions begin, some of the Cr(VI) ions can be converted into Cr(III) ions through oxidation of the organic compositions. The Cr(III) content remaining in the suspension is controlled by two factors: (i) the amount of Cr(VI) being reduced and (ii) the amount of Cr(III) sorbed on the negatively charged sites (i.e.,−COO^-) of WPWS. In this study, however, about 2−18% of the Cr(III) remained in the liquid phase when the sorption reactions were ending (Table 1). The Cr(III) content increases with increasing operating temperature and decreases with increasing initial Cr(VI) concentration. Nevertheless, the remaining content of Cr(III) seems to be independent of the particle size of WPWS. The value of Cr(T) removal increases nearly in proportion to the amount of remaining Cr(III) for different concentration treatments, and similar trends can also be observed for different temperature treatments except for particle size (Table 1). This result implies that the formation of Cr(III) is the limiting step for Cr removal, rather than just the adsorption of Cr(VI) without any reaction.

Effects of Temperature. Time profiles of the Cr(T) and Cr(VI) concentrations of WPWS at different temperatures are shown in Figure 3a and b, respectively. C_0 denotes the initial Cr(T) or Cr(VI) concentration in the aqueous phase (mg L^{-1}), and C_t denotes the Cr species concentration in the liquid phase at time t. The value of C_t/C_0 can be considered as an indication of Cr removal. It is well-known that reduction of Cr(VI) by organic materials is favored at higher temperature condition. The amounts of Cr(T) removed after treatments at 10, 30, and 50 °C are about 14%, 18%, and 25%, respectively. It is worth mentioning that the 10 °C treatment yields the lowest Cr(T) removal and remaining Cr(III) in this study (Table 1). These values are comparable to several literature results reported for various biosorbents (Table 2). The sorption capacities obtained with WPWS are significantly lower than those of other biosorbents. We consider that the low capacity for Cr removal was due to the dissolution of basic materials (i.e., Ca and Mg) from the WPWS during the reaction. Finally, the pH of the suspensions rose to 4.2. This should weaken protonation as well as the oxidation−reduction reaction and lead to a considerable decrease in Cr removal. However, studies of other biosorbents have not mentioned that the pH of the solutions fluctuated distinctly during sorption.[16−25] According to the kinetic model, all different temperature treatments show good compliance with a pseudo-second-order equation (Figure 4a,b), and the calculated sorption rate constants, k_2, for the 10, 30, and 50 °C treatments are 0.032, 0.068, and 0.072 g mg^{-1} min^{-1}, respectively (Table 3).

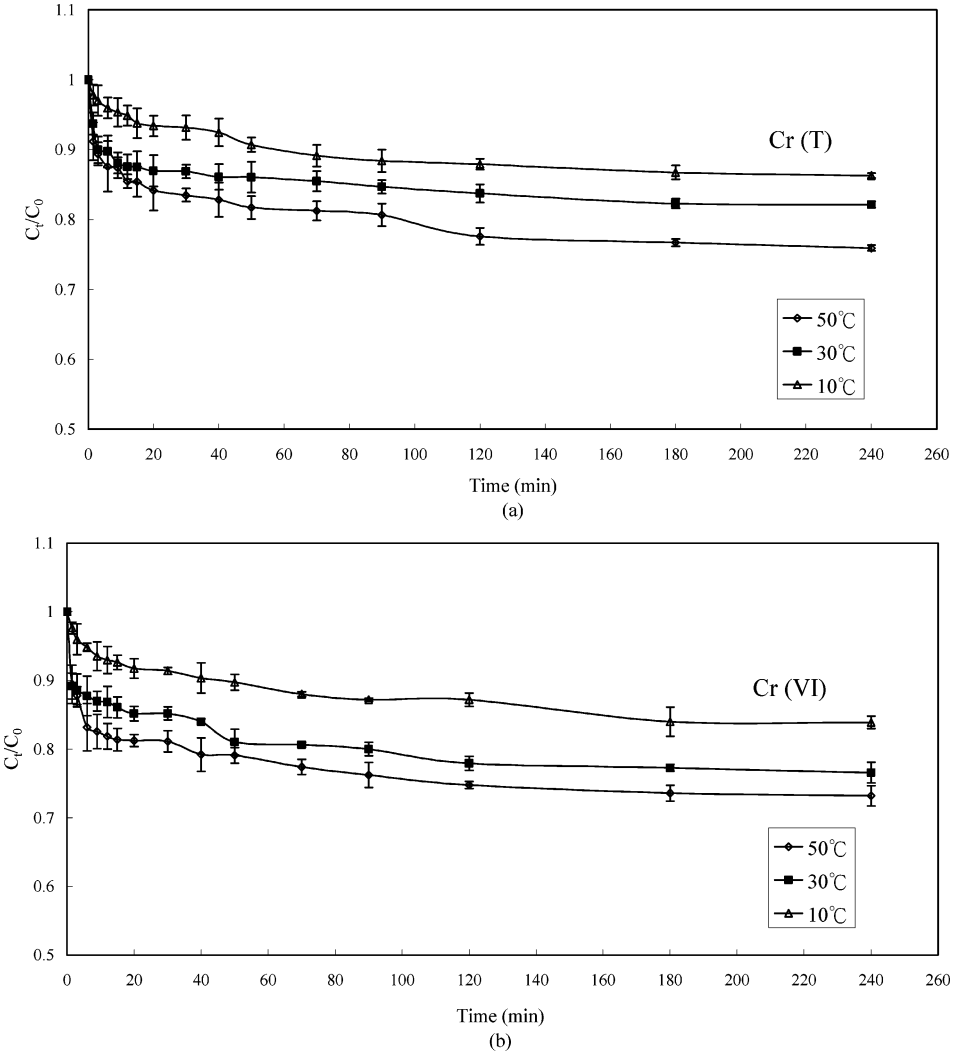

Figure 3. Time profiles of (a) Cr(T) and (b) Cr(VI) removal by WPWS at different operating temperatures (C_0 = 0.1 g L^{-1}, dosage = 10 g L^{-1}, 100−140 mesh, initial pH = 2.0). Error bars represent ±1 standard error.

Table 2. Adsorption Capacities of Various Adsorbents for Cr(VI)

biosorbent	pH	temp (°C)	maximum adsorption capacity (mg g^{-1})	ref
green algae *Spirogyra* species	2.0	18	14.7	22
pine needles	2.0	room	5.4	20
wheat bran	2.0	room	35.0	19
Lentinus sajor-caju	2.0	25	32.2	23
seed of *Ocimum basilicum*	1.5	25	205.0	17
rice bran	2.0	30	294.1	16
Chlamydomonas reinhardtii	2.0	25	18.2	24
Mucor hiemalis	2.0	27	47.4	25
eucalyptus bark	2.0	32	45.0	18

Effects of Initial Cr(VI) Concentration. The efficiency of removal of Cr(T) for WPWS follows the trend of 25 mg L^{-1} (36%) > 50 mg L^{-1} (24%) > 75 mg L^{-1} (21%) > 100 mg L^{-1} (18%) (Table 1). As shown in Figure 5a, the Cr removal is much better for the treatment of a 25 mg L^{-1} solution than for the other concentrations. The experimental data show that higher determination constants (R^2) fit the pseudo-second-order equation better than the pseudo-first-order model (Figure 5b and Table 3). The calculated pseudo-second-order sorption rate constants, k_2, for 25, 50, 75, and 100 mg L^{-1} Cr(VI) solutions are 0.084, 0.079, 0.071, and 0.069 g mg^{-1} min^{-1}, respectively. Increasing the Cr(VI) concentration in the suspension seems to reduce the diffusion of the Cr species in the boundary layer of the WPWS solid, which decreases the sorption rate.

Effects of Particle Size. The final Cr(T) removals for WPWS mesh sizes of 50−100, 100−140, 140−200, and >200 were 17%, 18%, 19%, and 22%, respectively (Table 1). There were only small differences in Cr(T) removal between various particle sizes (Figure 6a). It is proposed that the aggregates of WPWS gradually broke into small sizes when vigorously mixed in suspensions. The pseudo-second-order equation shows a better correlation (R^2 ranged from 0.979 to 0.998) than the pseudo-first-order equation (R^2 ranged from 0.914 to 0.975) (Figure 6b and Table 3). Thus, only the pseudo-second-order equation was employed for the kinetic study of the effect of particle size. The calculated sorption rate constants, k_2 (g mg^{-1} min^{-1}), for the pseudo-second-order equation increased with decreasing particle size, being 0.034, 0.069, 0.070, and 0.074 for the 50−100, 100−140, 140−200, and >200 mesh samples, respectively. In general, increasing particle size of the WPWS results in slightly lower sorption and removal rates.

X-ray Absorption Spectroscopic Studies. As depicted in Figure 7, an apparent preedge peak of $K_2Cr_2O_7$ appears near an absorption energy of 5993 eV, but all of the contour shapes of Cr-loaded WPWS samples are similar to that of $Cr(NO_3)_3$, which does not have noticeable preedge peak characteristics in its XANES spectrum. That is, Cr(VI) cannot be detected in our

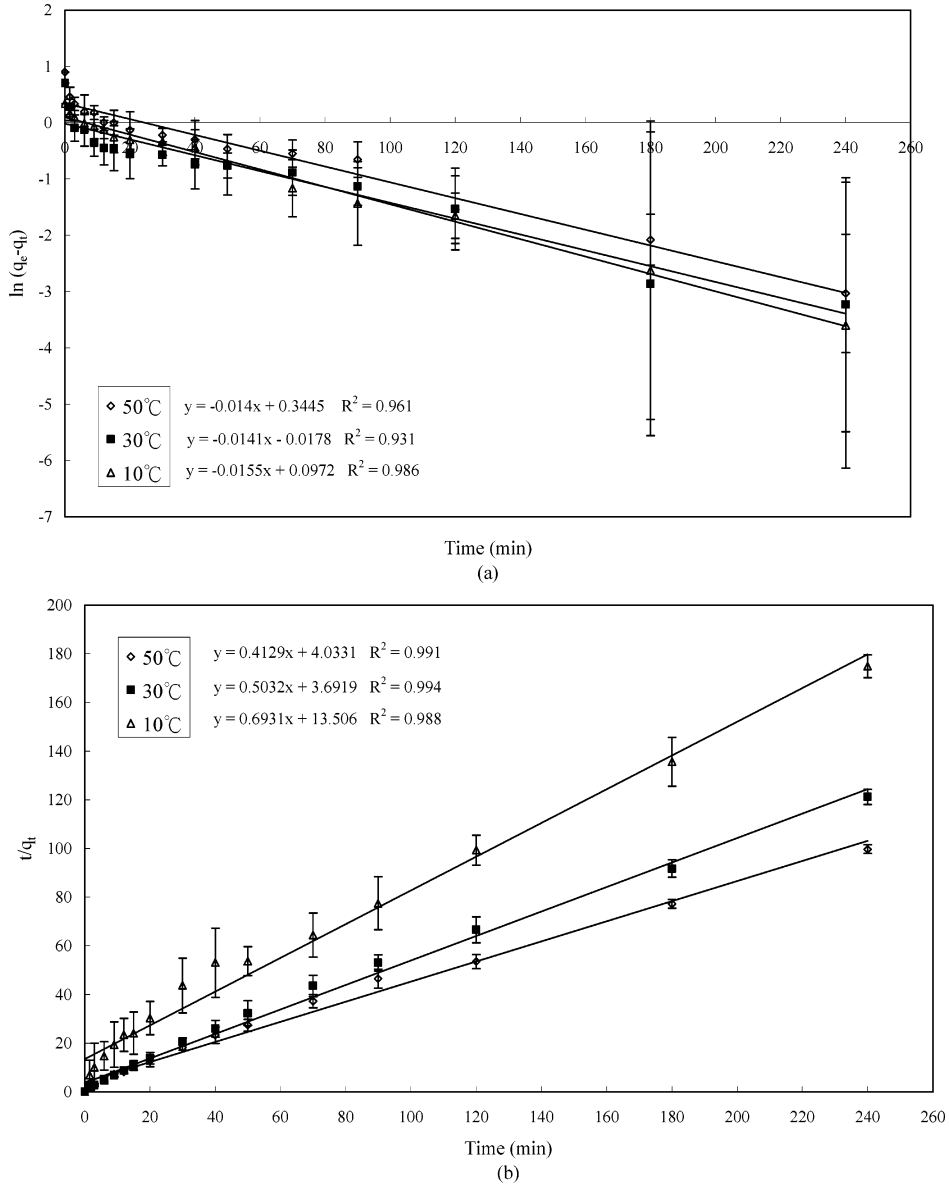

Figure 4. (a) Pseudo-first-order and (b) pseudo-second-order kinetic models of Cr(T) sorption by WPWS at different operating temperatures (C_0 = 0.1 g L^{-1}, dosage = 10 g L^{-1}, 100−140 mesh, initial pH = 2.0). Error bars represent ±1 standard error.

Table 3. Determination Constants (R^2) and Rate Constants of Pseudo-Second-Order (k_2) Models at Different Temperatures, Initial Cr(VI) Concentrations, and Particle Sizes of WPWS

	R^2		Rate Constants	
	first order	second order	k_1 (min^{-1})	k_2 (g mg^{-1} min^{-1})
Temperature				
10 °C	0.986	0.988	0.016	0.032
30 °C	0.931	0.994	0.014	0.068
50 °C	0.961	0.991	0.014	0.072
Concentration				
25 mg L^{-1}	0.957	0.989	0.015	0.084
50 mg L^{-1}	0.930	0.993	0.015	0.079
75 mg L^{-1}	0.963	0.994	0.014	0.071
100 mg L^{-1}	0.931	0.994	0.014	0.069
Particle Size				
50−100 mesh	0.975	0.979	0.015	0.034
100−140 mesh	0.931	0.994	0.014	0.069
140−200 mesh	0.933	0.996	0.013	0.070
>200 mesh	0.914	0.998	0.014	0.074

samples. The reduction rate of Cr(VI) is so high that Cr(III) can be observed at a reaction time of 1.5 min. Nevertheless, it is difficult to judge whether the sorbed Cr(VI) ions are reduced to Cr(III) ions in situ entirely or are completely washed away from the WPWS during sample preparation. Thus, the simple binding of Cr(VI) ions on the protonated functional groups is not the only way for WPWS to remove Cr(VI) from aqueous solutions. During reaction, many Cr(VI) ions approach the positively charged sites of WPWS and then are reduced to Cr(III) ions by the organic functional groups of WPWS and subsequently adsorbed by available negatively charged sites of WPWS and/or translocated into the liquid phase. Cr(VI) is known to be reduced by organic functional groups such as phenols, alcohols, and carboxylic acids, commonly found in humic substances.[7] However, non-humic organic substances such as carbohydrates and proteins also reduce Cr(VI).[44] Nakano et al.[27] proposed that Cr(VI) could be reduced to Cr(III) by tannin gel and that the Cr(III) ions could bind with carboxyl and/or hydroxyl groups via electrostatic interaction. At pH <4.2, the number of positively charged sites on WPWS is not sufficient to bind all of the Cr(III) ions. This explains why quantities of Cr(III) ions remain in the liquid phase. Extended

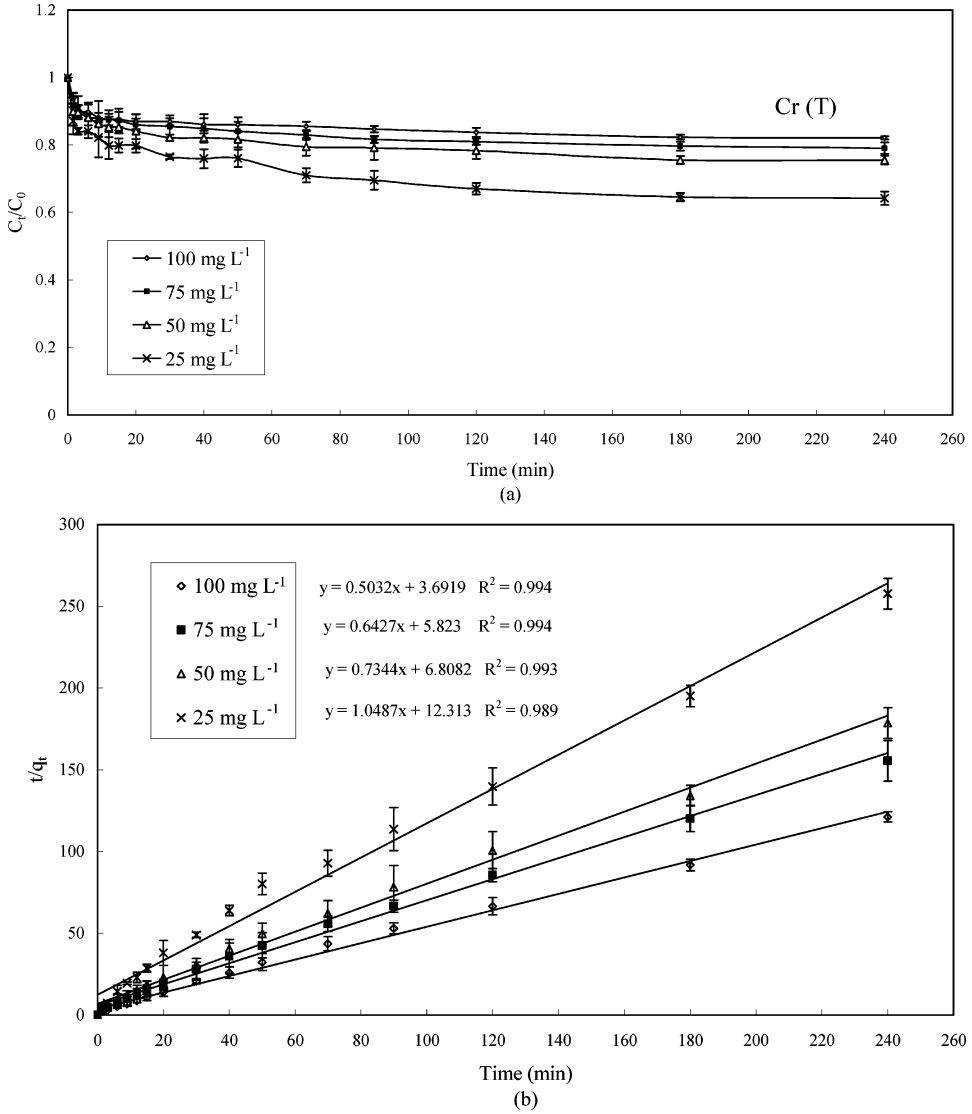

Figure 5. (a) Time profiles and (b) pseudo-second-order kinetic model of Cr(T) sorption by WPWS with different initial Cr(VI) concentrations (dosage = 10 g L^{-1}, 100−140 mesh, T = 30 °C, initial pH = 2.0). Error bars represent ±1 standard error.

X-ray absorption fine structure (EXAFS) can be employed to provide further information about the coordination environment, the nearest-neighbor atoms, and the ligands that are involved in the binding of Cr,[31] but there are limitations for complex materials such as sludge.[33] In addition, the presence of manganese, originating from the WPWS, interferes with the analysis of EXAFS data, because its K-edge energy (6539 eV) is just within the range of 6080−6989 eV. Gardea-Torresdey et al.[45] demonstrated that reduced Cr(III) is possibly bound to the oxygen-containing ligands of carboxyl groups of oat biomass, rather than the nitrogen ligands of amino groups from EXAFS studies.

Conclusions

WPWS is composed abundant labile carbohydrates. Carboxyl is the most important functional group interacting with chromium. All kinetic data obtained from different treatments show good compliance with a pseudo-second-order model. Increasing the Cr(VI) concentration seems to reduce the diffusion rate of metal ions in the boundary layer of WPWS, which decreases the adsorption rate. The mechanism of removal of Cr by WPWS is quite different from that of other biosorbents. The reduction rate of Cr(VI) is so high that the reduced form of Cr(III) can be observed on WPWS after 1.5 min by XANES. Thus, we suggest that the potential for Cr(VI) reduction to Cr(III) is the key factor affecting Cr removal in WPWS studies. Because the pH increases upon dissolution of basic materials, both protonation and the oxidation−reduction reaction decrease, leading to low Cr removal. Nevertheless, the formation of Cr(III) in suspensions indicates that the toxicity of the initial Cr(VI) solutions has been reduced already. We suggest that increasing the amount of WPWS used and maintaining the pH of suspension around 2.0 can enhance the removal of Cr when WPWS is applied in wastewater treatment. For EXAFS analysis, the interference from manganese needs to be overcome. Thus, Cr(III) coordination to WPWS and improvement in Cr removal merit further study.

Acknowledgment

This work was financially supported by the National Science Council, Taiwan, Republic of China, under Projects NSC 88-2313-B002-279, 89-2313-B002-279, 89-2621-B02-006, and 90-2313-B002-279.

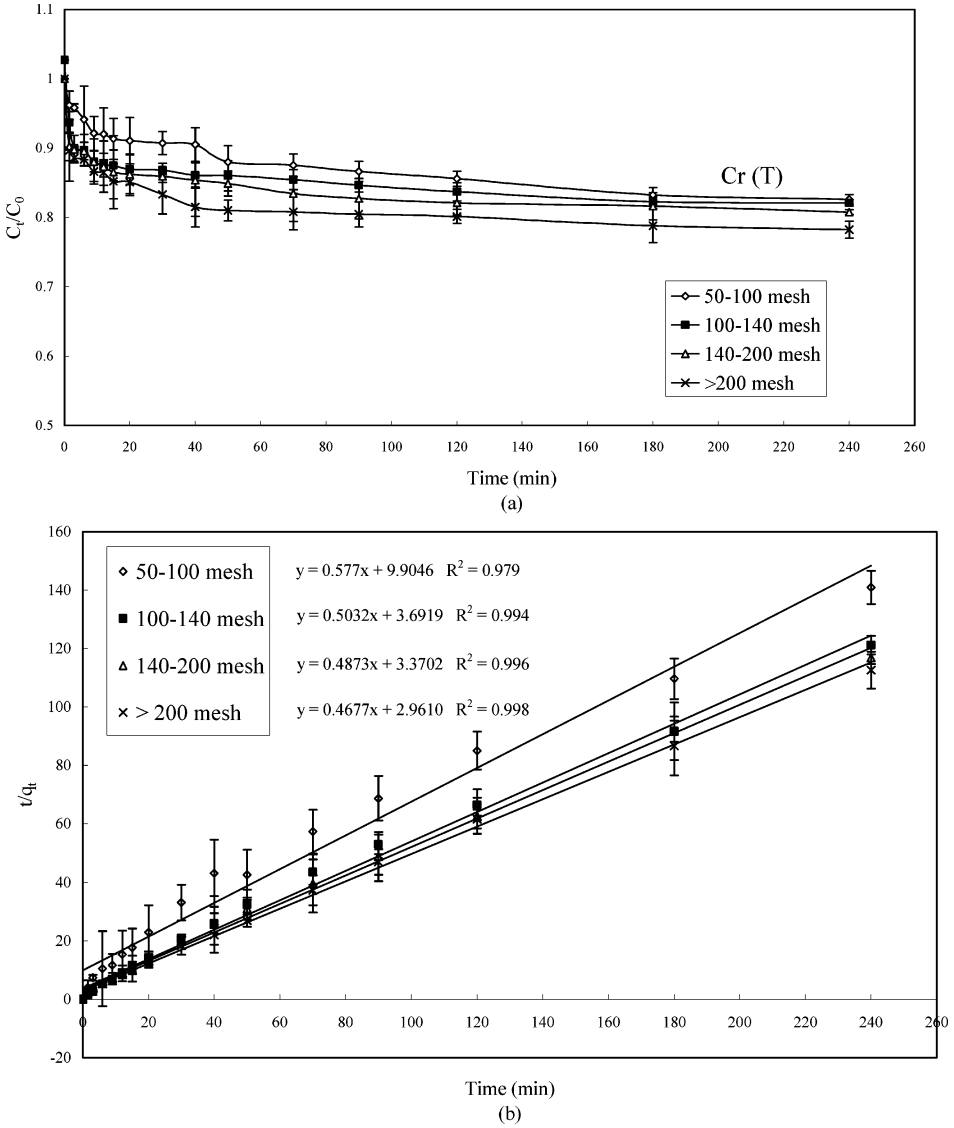

Figure 6. (a) Time profiles and (b) pseudo-second-order kinetic model of Cr(T) sorption by WPWS with different particle sizes (C_0 = 0.1 g L^{-1}, dosage = 10 g L^{-1}, T = 30 °C, initial pH = 2.0). Error bars represent ±1 standard error.

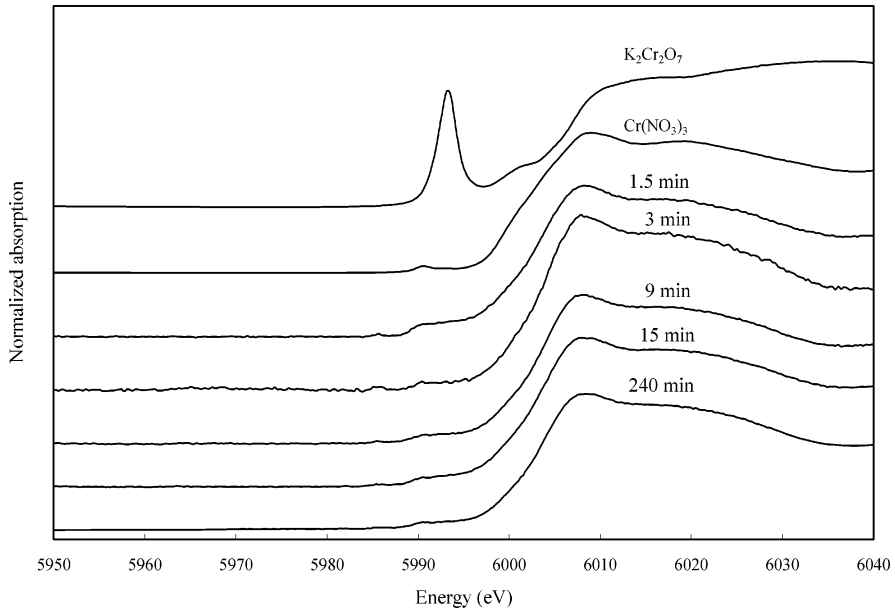

Figure 7. X-ray absorption near-edge spectra (XANES) of $K_2Cr_2O_7$, $Cr(NO_3)_3$, and WPWS sorbed Cr sampled at different time (100 mg L^{-1} Cr, 30 °C, initial pH = 2.0).

Literature Cited

(1) Lien, T. F.; Wu, C. P.; Lu, J. J.; Chou, R. G. R. Effects of supplemental chromium picolinate on growth performances, serum traits and characteristics of pigs. *Poult. Sci.* **1996**, *60*, 617.

(2) Kowalski, Z. Treatment of chromic tannery wastes. *J. Hazard. Mater.* **1994**, *37*, 137.

(3) Brigatti, M. F.; Franchini, G.; Lugli, C.; Medici, L.; Poppi, L.; Turci, E. Interaction between aqueous chromium solutions and layer silicates. *Appl. Geochem.* **2000**, *15*, 1307.

(4) Muthukumran, K.; Balasubramanian, N.; Ramakrushna, T. V. Removal and recovery of chromium from plating waste using chemically activated carbon. *Met. Finish.* **1995**, *93*, 46.

(5) Hunsoma, F.; Pruksathorn, K.; Damronglerd, S.; Vergnes, H.; Duverneuil, P. Electrochemical treatment of heavy metals (Cu^{2+}, Cr^{6+}, Ni^{2+}) from industrial effluent and modeling of copper reduction. *Water Res.* **2005**, *39*, 610.

(6) Hafez, A.; El-Manharawy, S. Design and performance of the two-stage/two-pass RO membrane system for chromium removal from tannery wastewater. Part 3. *Desalination* **2004**, *165*, 141.

(7) Palmer, C. D.; Wittbrodt, P. R. Processes affecting the remediation of chromium-contaminated sites. *Environ. Health Perspect.* **1991**, *92*, 25.

(8) Srivastava, S. K.; Gupta, V. K.; Mohan, D. Kinetic parameters for the removal of lead and chromium from wastewater using activated carbon developed from fertilizer waste material. *Environ. Model. Assess.* **1996**, *1*, 281.

(9) Lee, S. M.; Davis, P. A. Removal of Cu(II) and Cd(II) from aqueous solution by seafood processing waste sludge. *Water Res.* **2001**, *35*, 534.

(10) Gupta, V. K.; Ali, I. Removal of lead and chromium from wastewater using bagasse fly ash—A sugar industry waste. *J. Colloid Interface Sci.* **2004**, *271*, 321.

(11) Gupta, G. S.; Prasad, G.; Singh, V. N. Removal of chrome dye from aqueous solutions by mixed adsorbents: Fly ash and coal. *Water Res.* **1990**, *24*, 45.

(12) Stasinakis, A. S.; Thomaidis, N. S.; Mamais, D.; Karivali, M.; Lekkas, T. D. Chromium species behaviour in the activated sludge process. *Chemosphere* **2003**, *52*, 1059.

(13) Patnaik, L. N.; Das, C. P. Removal of hexavalent chromium by blast furnace fueldust. *Ind. J. Environ. Health* **1995**, *37*, 19.

(14) Gupta, V. K.; Gupta, M.; Sharma, S. Process development for the removal of lead and chromium from aqueous solutions using red mud-an aluminum industry waste. *Water Res.* **2001**, *35*, 1125.

(15) Selvaraj, K.; Manonmani, S.; Pattabhi, S. Removal of hexavalent chromium using distillery sludge. *Bioresour. Technol.* **2003**, *89*, 207.

(16) Singh, K. K.; Rastogi, R.; Hasan, S. H. Removal of Cr(VI) from wastewater using rice bran. *J. Colloid Interface Sci.* **2005**, *290*, 61.

(17) Melo, J. S.; D'Souza, S. F. Removal of chromium by mucilaginous seeds of *Ocimum. basilicum*. *Bioresour. Technol.* **2004**, *92*, 151.

(18) Sarin, V.; Pant, K. K. Removal of chromium from industrial waste by using eucalyptus bark. *Bioresour. Technol*. **2006**, *97*, 15.

(19) Dupont, L.; Gallon, E. Removal of hexavalent chromium with a lignocellulosic substrate extracted from wheat bran. *Environ. Sci. Technol.* **2003**, *37*, 4235.

(20) Dakiky, M.; Khamis, M.; Manassra, A.; Mer'eb, M. Selective adsorption of chromium(VI) in industrial wastewater using lowcost abundantly available adsorbents. *Adv. Environ. Res.* **2002**, *6*, 533.

(21) Sun, G.; Shi, W. Sunflower stalks as adsorbents for the removal of metal ions from wastewater. *Ind. Eng. Chem. Res.* **1998**, *37*, 1324.

(22) Gupta, V. K.; Shrivastava, A. K.; Jain, N. Biosorption of chromium-(VI) from aqueous solutions by green algae *Spirogyra* species. *Water Res.* **2001**, *35*, 4079.

(23) Arica, M. Y.; Bayramoglu, G. Cr(VI) biosorption from aqueous solutions using free and immobilized biomass of *Lentinus sajor-caju*: Preparation and kinetic characterization. *Colloids Surf. A: Physicochem. Eng. Aspects* **2005**, *253*, 203.

(24) Arica, M. Y.; Tuzun, I.; Yalcın, E.; Ince, O.; Bayramoglu, G. Utilisation of native, heat and acid-treated microalgae *Chlamydomonas reinhardtii* preparations for biosorption of Cr(VI) ions. *Process Biochem.* **2005**, *40*, 2351.

(25) Tewari, N.; Vasudevan, P.; Guha, B. K. Study on biosorption of Cr(VI) by *Mucor hiemalis*. *Biochem. Eng. J.* **2005**, *23*, 185.

(26) Walkley, A.; Black, C. A. An experimentation of Detjareff method and a proposed modification of the chromic acid titration method. *Soil Sci.* **1934**, *37*, 29.

(27) Nakano, Y.; Takeshita, K.; Tsutsumi, T. Adsorption mechanism of hexavalent chromium by redox within condensed-tannin gel. *Water Res.* **2001**, *35*, 496.

(28) Park, D.; Yun, Y. S.; Jo, J. H.; Park, J. M. Mechanism of hexavalent chromium removal by dead fungal biomass of *Aspergillus niger*. *Water Res.* **2005**, *39*, 533.

(29) *Standard Methods for the Examination of Waste and Wastewater*, 16th ed.; American Public Health Association: Washington, DC, 1985.

(30) Wu, F. C.; Tseng, R. L.; Juang, R. S. Kinetic modeling of liquid-phase adsorption of reactive dyes and metal ions on chitosan. *Water Res.* **2001**, *35*, 613.

(31) Sawalha, M. F.; Gardea-Torresdey, J. L.; Parsons, J. G.; Saupe, G.; Peralta-Videa, J. R. Determination of adsorption and speciation of chromium species by saltbush (*Atriplex canescene*) biomass using a combination of XAS and ICP-OES. *Microchem. J.* **2005**, *81*, 122.

(32) Hamada, E.; Nagoshi, M.; Sato, K.; Matsuzaki, A.; Yamaji, T.; Kuroda, K. Microstructure of organic−inorganic composite coatings studied by TEM and XANES. *Sci. Technol. Adv. Mater.* **2003**, *4*, 475.

(33) Shaffer, R. E.; Cross, J. O.; Rose-Pehrsson, S. L.; Elam, W. T. Speciation of chromium in simulated soil samples using X-ray absorption spectroscopy and multivariate calibration. *Anal. Chim. Acta* **2001**, *442*, 295.

(34) Engemann, C.; Hormes, J.; Longen, A.; Dotz, K. H. An X-ray absorption near edge spectroscopy XANES study on organochromium complexes at the Cr K-edge. *Chem. Phys.* **1998**, *237*, 471.

(35) Cheng, N.; Wei, Y. L.; Hsu, L. H.; Lee, J. F. XAS study of chromium in thermally cured mixture of clay and Cr-containing plating sludge. *J. Electron Spectrosc. Related Phenom.* **2005**, *144*−*147*, 821.

(36) Pietro, M.; Paola, C. Thermal analysis for evolution of the organic matter evolution during municipal solid waste aerobic composting process. *Thermochim. Acta* **2004**, *413*, 209.

(37) Lopez-Capel, E.; Sohi, S. P.; Gaunt, J. L.; David, A. C.; Manning, D. A. C. Use of thermogravimetry−differential scanning calorimetry to characterize modelable soil organic matter fraction. *Soil Sci. Soc. Am. J.* **2005**, *69*, 136.

(38) Abou-Mesalam, M. M. Sorption kinetics of copper, zinc, cadmium and nickel ions on synthesized silico-antimonate ion exchanger. *Colloids Surf. A: Physicochem. Eng. Aspects* **2003**, *225*, 85.

(39) White, J. L.; Roth, C. B. Infrared spectrometry. In *Methods of Soil Analysis*, 2nd ed.; Klute, A., Ed.; Agronomy Monograph 9; ASA and SSSA: Madison, WI, 1982; Part 1.

(40) Ghoreishi, S. M.; Haghighi, R. Chemical catalytic reaction and biological oxidation for treatment of non-biodegradable textile effluent. *Chem. Eng. J.* **2003**, *95*, 163.

(41) Gardea-Torresdey, J. L.; Dokken, K.; Thiemann, K. J.; Parsons, J. G.; Ramos, J.; Pingitore, N. E.; Gamez, G. Infrared and X-ray absorption spectroscopic studies on the mechanism of chromium(III) blinding to alfalfa biomass. *Microchem. J.* **2002**, *71*, 157.

(42) Gerasimowicz, W. V.; Byler, D. M. Carbon-13 CPMAS NMR and FTIR spectroscopic studies of humic acids. *Soil Sci.* **1985**, *139*, 270.

(43) Reveille, V.; Mansuy, L.; Jarde, E.; Garnier-Sillam, E. Characterisation of sewage sludge-derived organic matter: lipids and humic acids. *Org. Geochem.* **2003**, *34*, 615.

(44) Bolan, N. S.; Thiagarajan, S. Retention and plant availability of chromium in soils as affected by lime and organic matter amendments. *Aust. J. Soil Res.* **2001**, *39*, 1091.

(45) Gardea-Torresdey, J. L.; Tiemann, K. J.; Armendariz, V.; Bess-Oberto, L.; Chianelli, R. R.; Rios, J.; Parsons, J. G.; Gamez, G. Characterization of Cr(VI) binding and reduction to Cr(III) by the agricultural byproducts of *Avena monida* (Oat) biomass. *J. Hazard. Mater.* **2000**, *80B*, 175.

Received for review July 26, 2006
Revised manuscript received October 17, 2006
Accepted October 18, 2006

IE060978Q